

RESEARCH

Open Access



IGFBP7 is a key component of the senescence-associated secretory phenotype (SASP) that induces senescence in healthy cells by modulating the insulin, IGF, and activin A pathways

Yesuf Siraj^{1,5†}, Domenico Aprile^{1†}, Nicola Alessio¹, Gianfranco Peluso⁴, Giovanni Di Bernardo^{1,6*} and Umberto Galderisi^{1,2,3,6*}

Abstract

Senescent cells exert their effects through the release of various factors, collectively referred to as the senescence-associated secretory phenotype (SASP). The SASP can induce senescence in healthy cells (secondary senescence), modulate immune system function, reshape the extracellular matrix, and facilitate cancer progression.

Among SASP components, certain factors act as key regulators in the induction of secondary senescence. In this study, we evaluated the role of IGFBP7, a crucial SASP component. Our results demonstrated that ROS-prostaglandin signaling is involved in the release of IGFBP7. Furthermore, neutralizing antibodies targeting IGFBP7 attenuated the SASP's pro-senescence activity. Cells incubated with IGFBP7 also entered a state of senescence.

The senescence induced by IGFBP7 appears to be mediated through three primary pathways. First, IGFBP7 can bind to insulin, thereby inhibiting its anti-senescence and pro-growth effects. In addition to this inhibitory effect on the insulin pathway, IGFBP7 may enhance IGFII pro-senescence signaling by promoting its interaction with IGF2R while blocking IGF1R. These activities are dependent on ERK and AKT signaling pathways. Finally, IGFBP7 and Activin A, both of which can induce cellular senescence, appear to regulate and inhibit each other, suggesting a compensatory mechanism to prevent excessive senescence. Notably, our preliminary data indicate that IGFBP7, in addition to blocking Activin A, may interact with its receptors and induce senescence via SMAD pathways.

Our findings highlight that IGFBP7, along with other members of the IGFBP family, plays a pivotal role in senescence-related signaling pathways. Therefore, IGFBP7 may serve as a potential target for anti-aging strategies aimed at reducing the burden of senescence on tissues and organs.

[†]Yesuf Siraj and Domenico Aprile equally contributed to the research.

*Correspondence:
Giovanni Di Bernardo
gianni.dibernardo@unicampania.it
Umberto Galderisi
umberto.galderisi@unicampania.it

Full list of author information is available at the end of the article



© The Author(s) 2024. **Open Access** This article is licensed under a Creative Commons Attribution-NonCommercial-NoDerivatives 4.0 International License, which permits any non-commercial use, sharing, distribution and reproduction in any medium or format, as long as you give appropriate credit to the original author(s) and the source, provide a link to the Creative Commons licence, and indicate if you modified the licensed material. You do not have permission under this licence to share adapted material derived from this article or parts of it. The images or other third party material in this article are included in the article's Creative Commons licence, unless indicated otherwise in a credit line to the material. If material is not included in the article's Creative Commons licence and your intended use is not permitted by statutory regulation or exceeds the permitted use, you will need to obtain permission directly from the copyright holder. To view a copy of this licence, visit <http://creativecommons.org/licenses/by-nc-nd/4.0/>.

Keywords Senescence, Secretome, SASP, IGFBP, Mesenchymal stromal cells

Introduction

Stressful events that impair cellular homeostasis can lead cells to permanent cell cycle arrest and acquisition of new functions, thus becoming senescent cells. Evolutionarily, senescence arose as an anti-cancer mechanism, since it arrests the proliferation of damaged cells. This benefit, however, may be overbalanced by negative outcomes. Senescent cells contribute to organismal aging and inflammation phenomena. In addition, if senescent cells are not quickly removed from tissues and organs by the macrophagic activity of immune cells, they can further promote inflammation and switch their activities from anti- to pro-tumor functions [1–4].

Senescent cells act through the release of several factors, collectively indicated as the senescence-associated secretory phenotype (SASP), which can induce senescence of healthy cells (secondary senescence), modulate the immune system function, reshape the extracellular matrix, and facilitate cancer advancement [5–7].

Each component of SASP may be involved in one or multiple of the above-reported tasks and act accordingly through a hierarchical pattern. For example, a few components may function as master deciders for the induction of secondary senescence. In this context, insulin growth factors (IGFs) and insulin growth factors binding proteins (IGFBPs), which are components of a biological mechanism preserved through evolution, described as a ‘conserved regulatory system for aging,’ can play a key role in the spreading of senescence [8–10]. Indeed, in a previous work, we evidenced a causative role for IGFBP4 and IGFBP5 in inducing senescence of mesenchymal stromal cells (MSCs) and fibroblasts. These findings align with meta-analysis of SASP produced by different types of senescent cells, which consistently detected the presence of IGFBP4 and IGFBP7 [10–12].

The IGFBP proteins act as modulators of IGFs activity by functioning as transporters within extracellular fluids, lengtheners of half-life, and regulators of their interaction with cognate receptors [8, 13]. The IGFBPs are classified according to their affinity for IGFs, IGFBP1 to IGFBP6 have high affinity for IGFs, while those with low affinity for IGFs are named IGFBP-related proteins (IGFBPrp) [13–15]. IGFBP7, also named IGFBPrp1, besides its low affinity for IGF proteins, can interact and modulate the functions of several other proteins. IGFBP7 can bind insulin growth factor receptor 1 (IGF1R) and can inhibit its interaction with IGF ligands. IGFBP7 has a strong affinity for Insulin and it has been suggested that it can inhibit Insulin binding to its receptor, even if these experiments were carried out with over-physiological IGFBP7 levels [13, 14, 16]. IGFBP7 can also bind and block the

Activin A activity, acting as a Follistatin-like protein [17–19]. Activins, which are components of the transforming growth factor beta (TGF- β) superfamily, are involved in many biological processes (such as inflammation, immunity, fibrosis, growth arrest, stem cell multipotency, etc.) and their activity is modulated by Follistatins, which bind and inhibit Activins [17, 18, 20].

Given the constant presence of IGFBP7 in SASP, we decided to evaluate if this protein may have a causative role in secondary senescence thus contributing to senescence spreading from senescent cells, directly affected by stressful agents, to healthy cells that turn senescent in the presence of SASP factors.

We selected MSCs as a cellular model because of their vital role within the body. MSCs are a heterogeneous cell population located in bone marrow, adipose tissue, and the stromal regions of various organs. This population includes stem cells, progenitor cells, fibroblasts, stromal cells, among others, and they play a key role by secreting growth and survival factors, immunomodulatory substances, and differentiation molecules, all of which support tissue repair and maintain overall homeostasis in the organism [21]. In this context, any senescence phenomenon affecting MSCs may greatly contribute to organismal aging.

Results

We treated MSCs with 300 μ M H₂O₂ to induce senescence and collected the SASP 72 h later. The H₂O₂ treatment resulted in a significant increase in senescent (Ki67-; β -galactosidase+) and stressed cells (Ki67+; β -galactosidase+), along with a decrease in cycling cells (Ki67+; β -galactosidase-) (Fig. 1A). We detected substantial amounts of IGFBP7 in the secretome of senescent cells, whereas its presence in the secretome of healthy cells was barely detectable (Fig. 1A).

Incubation of healthy MSCs with SASP from senescent cells induced secondary senescence, whereas the secretome produced by control cultures did not significantly alter the percentage of senescent cells (Fig. 1B). Pretreatment of SASP with an antibody targeting IGFBP7 markedly reduced SASP-induced secondary senescence (Fig. 1B). The serum level of IGFBP7 has been reported in several studies with significant discrepancies, ranging from less than 2 ng/ml to over 20 ng/ml [22, 23]. In light of this variability, we decided to incubate cells with a concentration higher than the maximum reported healthy serum value. Incubation of healthy MSCs with IGFBP7 alone induced senescence and cell cycle arrest, with no evidence of apoptosis (Fig. 1B, right histogram; Fig. 1C). The senescence process was associated with its

executive program, which in MSCs involves RB2 (P130), P53, CDKN1A (P21), and CDKN1B (P27) (Fig. 1D). It is important to mention that RB1-P16 has been demonstrated may play only a supporting role in the senescence of human MSCs. It is worthy to mention that BCL-2 and the P38MAPK, which are involved in blocking and promoting apoptosis, respectively [24], were both upregulated in IGFBP7 treated cells. This suggests that the absence of changes in apoptosis levels, as confirmed by ANXAV expression, may be due to a fine-tuned balance between pro- and anti-apoptotic pathways.

Senescence can significantly impact the stemness properties (self-renewal, lineage commitment, and undifferentiated status) of stem cells within MSCs. Indeed, we observed a marked decrease in key stemness factors [25, 26] in MSCs following incubation with IGFBP7 (Fig. 1D, right histogram). These findings collectively suggest that IGFBP7 may serve as a critical regulator in the induction of senescence.

Senescence signaling associated with IGFBP7 release

Senescent cells exhibit increased production of reactive oxygen species (ROS), which, in turn, promote the release of prostaglandins, contributing to the pro-inflammatory activity of the SASP [27–31]. In a previous study, we demonstrated that the surge in ROS in senescent cells promotes PGE2 release, and that these events are associated with IGFBP4 secretion [12].

Treatment of MSCs with H₂O₂, followed by incubation in medium containing antioxidants, affected the onset of senescence and significantly reduced IGFBP7 release (Fig. 1E). Furthermore, H₂O₂-treated cells, in the presence of a Cyclooxygenase-2 (COX-2) inhibitor, which reduces PGE2 production, did not exhibit significant IGFBP7 release, nor did they show an increase in the number of senescent cells (Fig. 1E).

IGFBP7-associated signaling involved in the induction of cellular senescence

What molecular partners does IGFBP7 engage to promote senescence? We investigated how the pro-senescence activity of IGFBP7 is modulated in the presence of its potential partners (Insulin, IGF1R, IGFII, Activin A) and the associated signaling pathways.

IGFBP7 and insulin

IGFBP7 has been suggested to bind Insulin and inhibit its activity [16]. As a preliminary step, we evaluated the pro-senescence effect of IGFBP7 in the presence of Insulin, which is known to reduce senescence [32–34].

Incubation of healthy MSCs with Insulin reduced the percentage of senescent cells to a negligible level and decreased the number of quiescent cells (Fig. 2A). This effect appears to occur primarily through the interaction

of Insulin with its receptors (INSR-A; INSR-B), as Insulin supplementation in the presence of antibodies targeting the alpha domain of these receptors did not reduce senescence or quiescence. In fact, it increased these phenomena compared to control cultures (Fig. 2A). This further increase in senescence, along with the observation that senescence is upregulated when cultures are supplemented only with antibodies targeting Insulin receptors, may be explained by the presence of a minimal amount of Insulin in the cell culture medium, even without additional supplementation.

The anti-senescence activity of Insulin was abolished by the presence of IGFBP7, supporting studies suggesting that IGFBP7 binds Insulin and blocks its interaction with cognate receptors (Fig. 2A). The literature data on the interaction between IGFBP7 and Insulin activity [16] were further validated by our immunoprecipitation experiments, which demonstrated a putative interaction between these two proteins (Fig. 2A).

IGFBP7 and IGF1R

There is evidence suggesting that IGFBP7 can bind IGF1R [35]. This receptor, along with IGF2R, is a binding partner of IGFII [36]. In a previous study, we demonstrated that IGFII induces senescence in MSCs primarily through binding to the IGF2R receptor, while the interaction of IGFII with IGF1R is not necessary for senescence induction. Specifically, supplementation of IGFII to MSCs in the presence of IGF1R-neutralizing antibodies further promoted senescence, as IGFII was fully redirected to IGF2R [12]. Studies also suggest that IGFBP7 may bind to and inactivate IGF1R [35]. A finding supported by our immunoprecipitation experiments (Fig. 2B).

We then investigated whether IGFBP7-induced senescence is related to this binding activity. MSCs treated with IGFII in the presence of IGFBP7 exhibited increased senescence compared to cells treated with IGFII alone (Fig. 2B). Senescence levels in cultures treated with IGFII and IGF1R-neutralizing antibodies were similar to those observed in IGFII/IGFBP7-treated samples, although the percentage of cycling cells was lower in the latter condition. Additionally, in samples incubated with IGFII/IGFBP7 and IGF1R-neutralizing antibodies, senescence levels were comparable to those in IGFII/IGFBP7-treated samples (Fig. 2B). Collectively, these data suggest that the senescence effect of IGFBP7 may be related to its binding activity with IGF1R and modulation of IGFII signaling.

ERK, AKT signaling and IGFBP7-induced senescence

Insulin and IGFII can transduce molecular signals through multiple kinase-associated pathways, depending on the intensity and duration of external stimuli, cell type, cell functional status, and intracellular context. In this complex scenario, identifying a single, specific

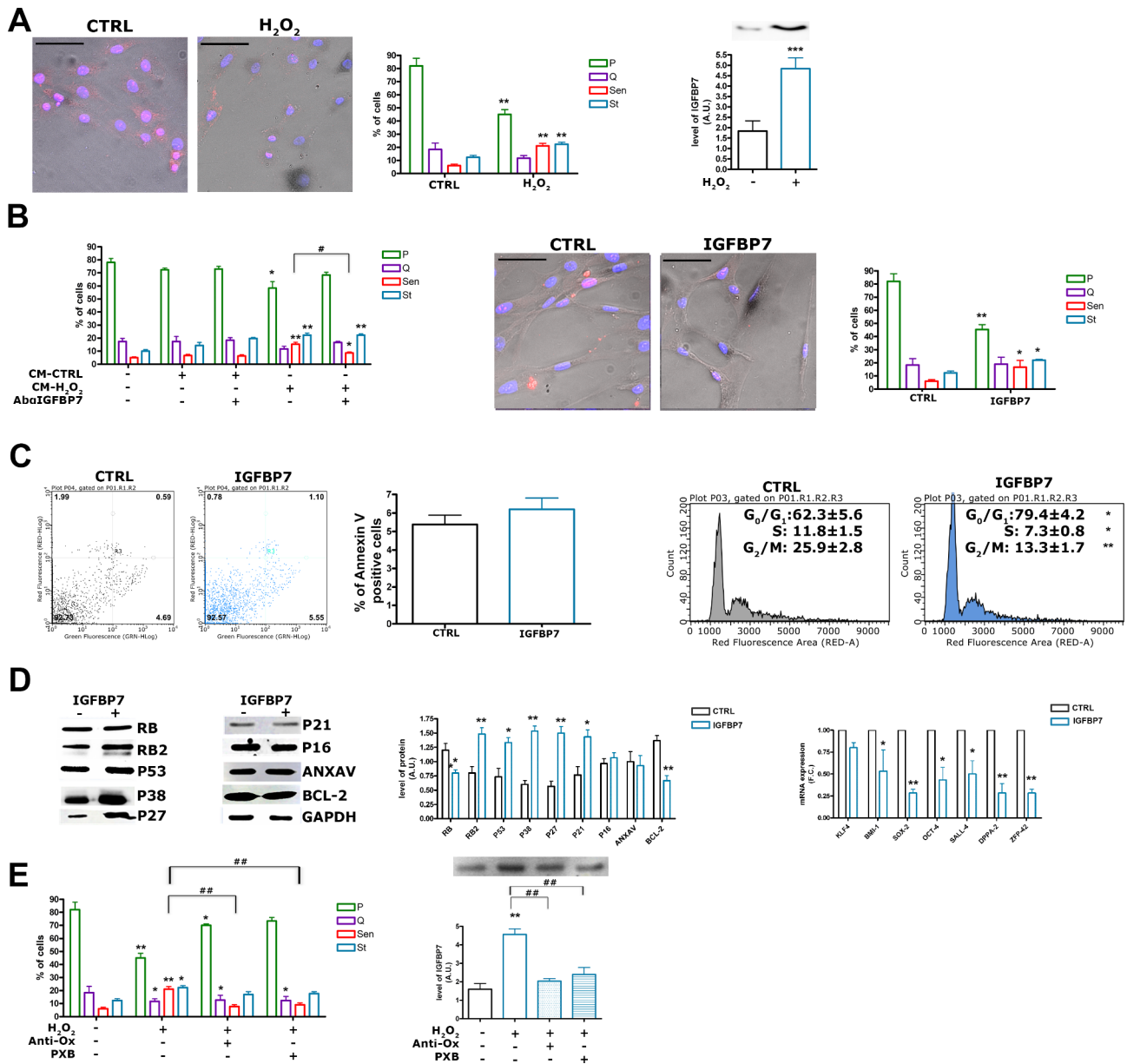


Fig. 1 (See legend on next page.)

signaling pathway involved in modulating senescence is challenging. However, previous investigations suggest that multiple senescence-inducing signals may converge on the ERK and AKT pathways. We evaluated the activation status of ERK1/2 and AKT in MSCs treated with IGFBP7 in combination with Insulin or IGFII. Initially, we examined whether the modulation of senescence by IGFBP7, Insulin, and IGFII was affected by blocking ERK and AKT signaling. The presence of U0126, a MEK inhibitor, or GSK-690,693, an AKT inhibitor, in the culture medium greatly impaired the pro-senescence activity of IGFBP7 (Fig. 2C). Similarly, the anti-senescence

function of Insulin also mainly depended on AKT pathway (Fig. 2C).

These biological findings were consistent with increased levels of activated ERK and AKT in the nuclei of cells treated with IGFBP7 and/or Insulin (Fig. 2D). The senescence induced by IGFII was also affected by the inhibition of ERK and AKT signaling, even if for this last pathway we did not evidence an increase of nuclear phosphorylated AKT (Fig. 2C and D).

IGFBP7 and activin A

The incubation of MSC cultures with Activin A resulted in an increased percentage of senescent and stressed

(See figure on previous page.)

Fig. 1 IGFBP7 and senescence. **(A)** On the left, the pictures show representative images of senescent (Ki-67⁻; β -galactosidase⁺) in healthy control samples (CTRL) and induced senescence (H₂O₂) samples. Cells were stained to identify nuclei (DAPI in blue), Ki67 (red), to evaluate β -galactosidase activity (dark gray). We used a Zeiss AxioScope 5 microscope, equipped with an Axicam 305 digital camera. The β -galactosidase activity was detected as a gray stain using this configuration. This method allowed us to identify cells that exhibited a visible light signal β -galactosidase along with others expressing fluorescent signals within the same cell. The black bar corresponds to 100 microns. The accompanying histogram shows the percentage of (P) cycling (Ki67⁺; β -galactosidase⁻), (Q) quiescent (Ki67⁻; β -galactosidase⁻), (St) stressed (Ki67⁺; β -galactosidase⁺), and (Sen) senescent (Ki67⁻; β -galactosidase⁺) cells three days following treatment with H₂O₂. Data are expressed with standard deviation (n=3 biological replicates). The symbol ***p*<0.01 indicate statistical significance between the control (CTRL) and H₂O₂ treated samples. At the top on the right, the picture shows a representative western blot analysis of IGFBP7 in MSCs secretome collected 72 h following H₂O₂ treatment and in controls. The histogram shows the protein levels expressed in arbitrary units (A.U.). Data are expressed with standard deviation (n=3 biological replicates). The symbol ****p*<0.001 indicate statistical significance between the control and H₂O₂ treated samples. **(B)** On the left, the histogram shows the percentage of (P) cycling (Ki67⁺; β -galactosidase⁻), (Q) quiescent (Ki67⁻; β -galactosidase⁻), (St) stressed (Ki67⁺; β -galactosidase⁺), and (Sen) senescent (Ki67⁻; β -galactosidase⁺) in MSCs incubated for 72 h either with secretome of healthy cells (CM-CTRL) or with secretome of H₂O₂ treated cells with and without supplementation of anti-IGFBP7 neutralizing antibodies (AbalIGFBP7). Data are expressed with standard deviation (n=3 biological replicates). The symbols ***p*<0.01 and **p*<0.05 indicate statistical significance between the control (CTRL) and treated samples. The symbol #*p*<0.05 indicates statistical significance between the CM-H₂O₂ sample, chosen as a reference, and CM-H₂O₂ + AbalIGFBP7. On the middle, the pictures show representative images of senescent (Ki-67⁻; β -galactosidase⁺) in healthy control samples (CTRL) and samples incubated with IGFBP7. Cells were stained to identify nuclei (DAPI in blue), Ki67 (red), to evaluate β -galactosidase activity (dark gray). The black bar corresponds to 100 microns. The accompanying histogram shows the percentage of (P) cycling, (Q) quiescent, (St) stressed, and (Sen) senescent. Data are expressed with standard deviation (n=3 biological replicates). The symbols ***p*<0.01 and **p*<0.05 indicate statistical significance between the control (CTRL) and treated samples. **(C)** On the left, Flow cytometry chart of Annexin V assay on healthy MSCs (CTRL) and in cells incubated with IGFBP7. The percentage of detected apoptotic cells is reported in the histogram. On the right, Cell cycle plots of healthy (CTRL) and IGFBP7 treated MSCs. Data are expressed with standard deviation (n=3 biological replicates). For every cell cycle phase, the symbols **p*<0.05 and ***p*<0.01 indicate the statistical difference between the CTRL samples and those treated with IGFBP7. **(D)** On the left, representative western blot analysis carried out on healthy (CTRL) and IGFBP7 treated MSCs. The accompanying histogram shows the protein levels expressed in arbitrary units (A.U.). GAPDH was used to normalize protein expression levels. Data are expressed with standard deviation (n=3 biological replicates). The symbols ***p*<0.01 and **p*<0.05 indicate statistical significance between the control (CTRL) and treated samples. On the right, the histogram shows the mRNA levels of the indicated genes, which were expressed in arbitrary units (A.U.). GAPDH was used to normalize mRNA expression levels. Data are expressed with standard deviation (n=3 biological replicates). The symbols ***p*<0.01 and **p*<0.05 indicate statistical significance between the control (CTRL) and treated samples. **(E)** On the left, the histogram shows the percentage of (P) cycling, (Q) quiescent, (St) stressed, and (Sen) senescent cells three days following H₂O₂ treatment with/without Anti-oxidant supplement (Anti-Ox) or with/without Parecoxib (PXB). Data are expressed with standard deviation (n=3 biological replicates). The symbols ***p*<0.01 and **p*<0.05 indicate statistical significance between the control and treated samples. The symbol ##*p*<0.01 represents statistical significance between the indicated samples. On the right, IGFBP7 expression level in the secretome of cells treated as above reported. At the top of histogram, a representative western blot image of IGFBP7 protein expression. Data are expressed with standard deviation (n=3 biological replicates). The symbol ***p*<0.01 represents statistical significance between the control and treated samples. The symbol ###*p*<0.01 represents statistical significance between the indicated samples

cells, accompanied by a decrease in the number of cycling cells. Stressed cells may either recover from the stress stimuli or progress to an irreversible senescent state (Fig. 3A). This finding aligns with studies indicating that Activin A, a component of the SASP, can promote cell cycle arrest [6, 17, 37]. Notably, co-supplementation of IGFBP7 and Activin A almost completely abolished the pro-senescence effects of both molecules, suggesting mutual inhibition (Fig. 3A). Supporting this hypothesis, there is evidence that IGFBP7 may function similarly to Follistatin, binding Activin A and inhibiting its interaction with receptors [19]. Our co-immunoprecipitation analysis further supports this hypothesis (Fig. 3A).

Activins exert their functions through interactions with specific type I and type II receptor complexes, which subsequently activate Smad proteins. To date, three type I receptors (ACVR1, ACVR1B, ACVR1C) and two type II receptors (ACVR2A, ACVR2B) have been identified [38]. Activins bind to one of the type II receptors, inducing the recruitment of a type I receptor. Activin A preferentially binds to ACVR1 or ACVR1B [39]. We evaluated the pro-senescence activity of Activin/IGFBP7 in the presence of neutralizing antibodies against ACVR1 or ACVR1B (Fig. 3A).

Inhibition of ACVR1 slightly decreased the pro-senescence effect of Activin A, although this reduction was not statistically significant. In contrast, blocking ACVR1B significantly reduced the senescence induced by Activin A treatment (Fig. 3A). Interestingly, IGFBP7 appeared to rely on both ACVR1 and ACVR1B to induce senescence (Fig. 3A). These biological results align with the activation of SMAD2/3 and SMAD1/5 signaling pathways (Fig. 3B). Specifically, IGFBP7 signaling involved both SMAD1/5 and SMAD2/3, whereas Activin A primarily engaged SMAD2/3. The literature supports that ACVR1 signals through SMAD1/5/8, while ACVR1B signals through SMAD2/3 [40].

The observation that blocking ACVR1 and ACVR1B impairs IGFBP7's pro-senescence effect prompted us to conduct preliminary analyses on the potential interaction of IGFBP7 with these receptors. An immunoprecipitation experiment provided evidence of a putative interaction between IGFBP7 and both ACVR1 and ACVR1B (Fig. 3C). This hypothesis was further supported by the Duolink[®] Proximity Ligation Assay, which enables the microscopic detection of protein-protein interactions by emitting a fluorescent signal for each interaction event.

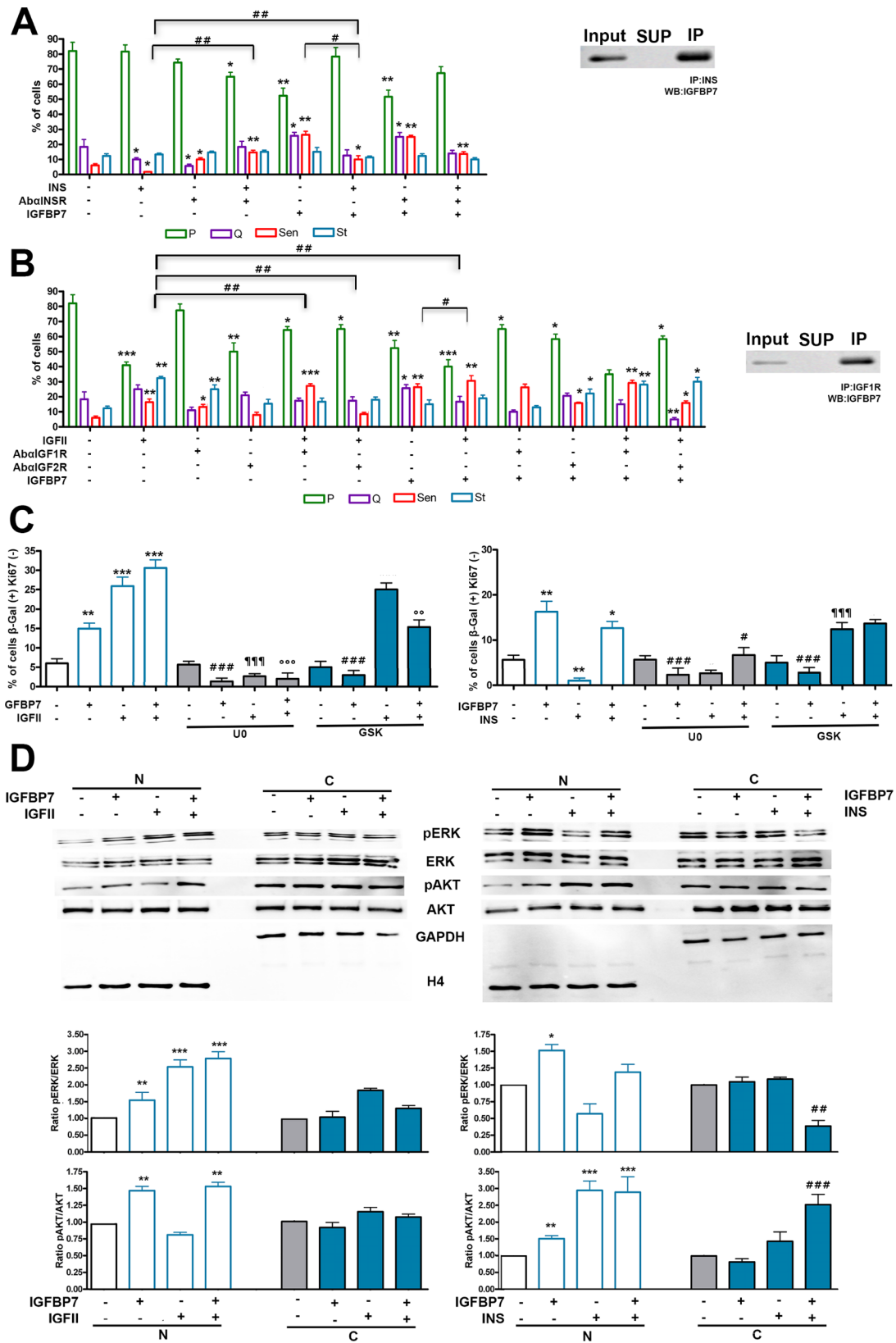


Fig. 2 (See legend on next page.)

(See figure on previous page.)

Fig. 2 IGFBP7 and its molecular partners. **(A)** Insulin and IGFBP7. The histogram shows the percentage of (P) cycling, (Q) quiescent, (St) stressed, and (Sen) senescent cells in MSCs cultures incubated with Insulin (INS) and/or IGFBP7 and/or antibodies targeting Insulin receptors (AbalNSR). Data are expressed with standard deviation ($n=3$ biological replicates). The symbol $**p < 0.01$ represents statistical significance between the control and treated samples. The symbols $##p < 0.01$ and $\#p < 0.05$ represent statistical significance between the indicated samples. On the right, immunoprecipitation experiment performed on culture medium containing both IGFBP7 and Insulin. The proteins were immunoprecipitated with anti-IGFBP7 antibody and western blot was performed with anti-Insulin antibody. Input: western blot performed on proteins present in medium; SUP and IP indicate the supernatant and the immunoprecipitated components of immunoreaction, respectively. **(B)** IGFII and IGFBP7. The histogram shows the percentage of (P) cycling, (Q) quiescent, (St) stressed, and (Sen) senescent cells in MSC cultures incubated with IGFII and/or IGFBP7 and/or antibodies targeting IGFII receptors (AbalGFR1, AbalGFR2). Data are expressed with standard deviation ($n=3$ biological replicates). The symbols $***p < 0.001$, $**p < 0.01$ and $*p < 0.05$ represent statistical significance between the control and treated samples. The symbols $##p < 0.01$ and $\#p < 0.05$ represent statistical significance between the indicated samples. On the right, immunoprecipitation experiment performed on secretome of cells incubated with IGFBP7. The proteins were immunoprecipitated with anti-IGFBP7 antibody and western blot was performed with anti-IGFR1 antibody. Input: western blot performed on proteins present in secretome; SUP and IP indicate the supernatant and the immunoprecipitated components of immunoreaction, respectively. **(C)** ERK and AKT pathways. The histograms show the percentage of senescent cells in MSCs cultures incubated with IGFBP7 and/or Insulin (INS), and/or IGFII, and/or U0126, a MEK inhibitor (UO), and/or GSK-690,693, an AKT inhibitor (GSK). Data are expressed with standard deviation ($n=3$ biological replicates). In the two histograms, the symbols on the white bars $**p < 0.01$ and $*p < 0.05$ represent a statistical significance between the control and treated samples. In the UO treated samples (grey bars): the symbol $###p < 0.001$ represents a statistical difference between the samples incubated with IGFBP7 with/without UO; the symbol $\#p < 0.05$ represents a statistical difference between samples incubated with IGFBP7 and insulin with/without UO; the symbol $¶¶¶p < 0.001$ represents a statistical difference between the samples incubated with IGFII with/without UO; the symbol $***p < 0.001$ represents a statistical difference between the samples incubated with IGFBP7 and IGFII with/without UO. In the GSK treated samples (blue bars): the symbol $###p < 0.001$ represents a statistical difference between the samples incubated with IGFBP7 with/without GSK; the symbol $°p < 0.01$ represents a statistical difference between the samples incubated with IGFBP7 and IGFII with/without GSK; the symbol $¶¶¶p < 0.001$ represents a statistical difference between the samples incubated with Insulin with/without GSK. **(D)** ERK and AKT pathways. Representative western blot analysis of nuclear and cytoplasmic levels of phosphorylated-ERK (pERK), ERK, phosphorylated-AKT (pAKT), AKT in cells incubated with IGFBP7 and/or Insulin and/or IGFII. GAPDH and Histone 4 (H4) were used as cytoplasmic and nuclear markers, respectively. The histograms show the cytoplasmic and nuclear pERK/ERK and pAKT/AKT ratios in the different experimental conditions. Data are expressed with standard deviation ($n=3$ biological replicates). In the histograms, the symbols on the white bars $***p < 0.001$ and $**p < 0.01$ represent a statistical significance between the control and treated samples; the symbols on the blue bars $###p < 0.001$ and $##p < 0.01$ represent a statistical significance between the control and treated samples

We observed a robust signal in MSCs cultured with IGFBP7 and either ACVR1 or ACVR1B (Fig. 3C).

Discussion

Senescence spreads from cells directly impacted by genotoxic stimuli to neighboring cells, primarily through the SASP, which plays a crucial role in both aging and cancer development. The SASP comprises various factors that regulate processes such as inducing secondary senescence, modulating immune system activity, remodeling the extracellular matrix, altering tissue structure, and sustaining cancer progression. Identifying these key molecules is essential for understanding the biological basis of senescence and for devising effective strategies to counteract it.

In this context, we evaluated the role of IGFBP7, a key SASP component, given its nearly ubiquitous presence in the secretome of senescent cells, irrespective of the stress inducer, duration, or cell type [10]. Our study indicates that ROS-prostaglandin signaling is part of the circuit involved in the release of IGFBP7. Conversely, incubation of healthy MSCs with IGFBP7 alone induced cell senescence, while in cultures treated with SASP containing IGFBP7-neutralizing antibodies, the induction of secondary senescence was greatly impaired.

Healthy MSCs treated with IGFBP7 also showed an increase in the percentage of stressed cells. Following a genotoxic stimulus, senescence-associated β -galactosidase, which operates optimally at pH 6.0, is

initially activated. However, its activity may decline if lysosomes successfully manage the stress. Alternatively, if the stress causes persistent damage to cellular structures (including DNA) that cannot be repaired, cells may enter a state of permanent senescence. Therefore, stressed cells may represent a metastable state, in which they either recover and revert to functional cells or progress towards senescence. In this context, cells treated with IGFBP7 may be gradually entering senescence.

These findings suggest that IGFBP7 exerts a paracrine effect by promoting senescence in healthy cells surrounding senescent cells. The ROS-prostaglandin signaling pathway appears to play a general role in the release of SASP factors, as our previous findings indicate that this pathway is also involved in IGFBP4 secretion, another component of the senescent secretome [12]. Moreover, other reports show that senescent cells synthesize and accumulate prostaglandins, which contribute to SASP release [41, 42].

The senescence induced by IGFBP7 appears to depend on three main pathways. First, IGFBP7 can bind to Insulin, thereby blocking its anti-senescence and pro-growth effects. In addition to this inhibitory effect on the Insulin pathway, IGFBP7 may positively modulate IGFII pro-senescence molecular circuits by shifting IGFII signaling to its IGF2R receptors while blocking IGF1R. These biological activities rely on ERK and AKT signaling. Finally, IGFBP7 and Activin A, both capable of inducing cellular senescence, can regulate and inhibit each other,

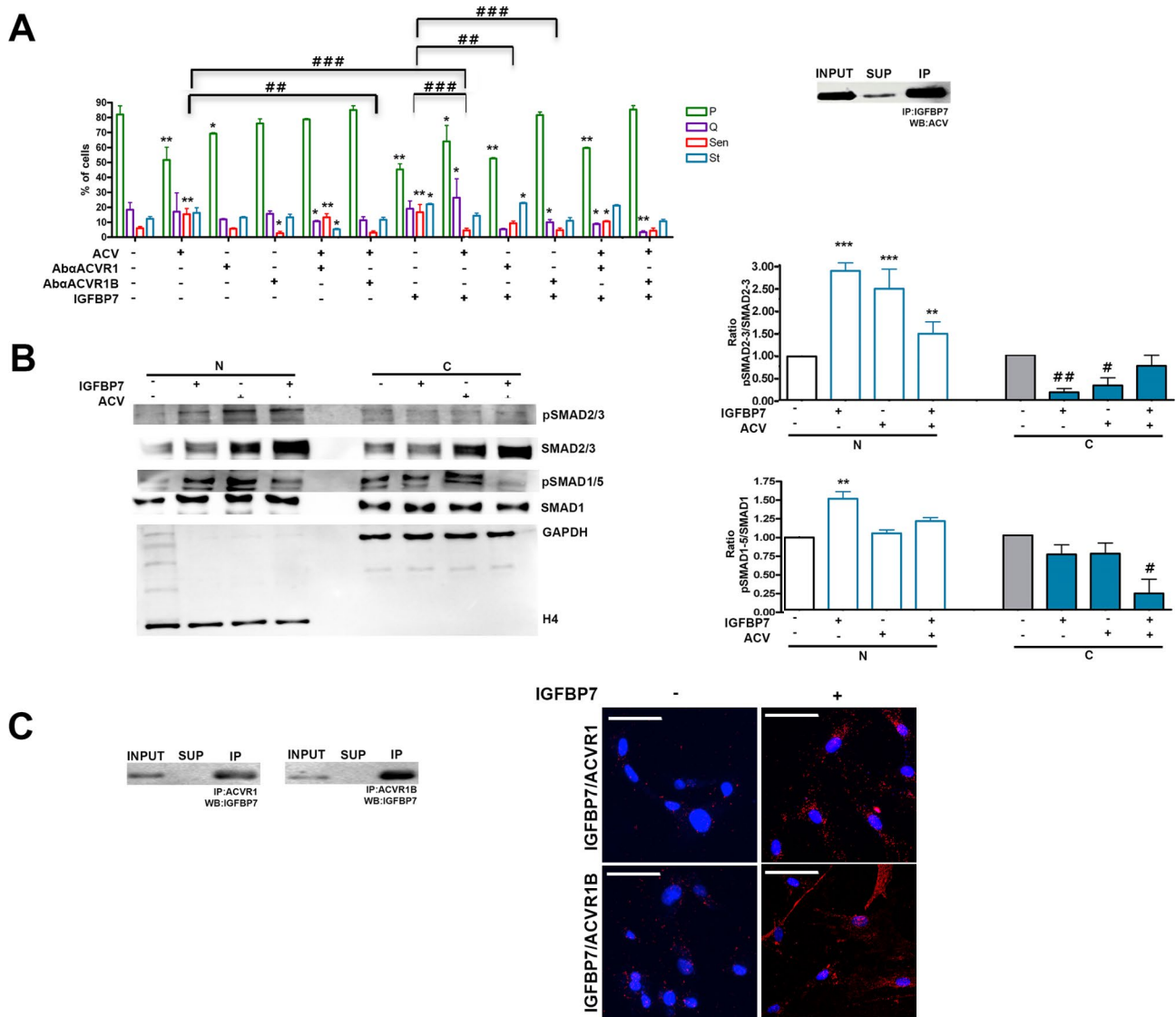


Fig. 3 IGFBP7 and Activin A. **(A)** The histogram shows the percentage of (P) cycling, (Q) quiescent, (St) stressed, and (Sen) senescent cells in MSCs cultures incubated with Activin A (ACV) and/or IGFBP7 and/or antibodies targeting Activin A receptors (AbaACVR1, AbaACVR1B). Data are expressed with standard deviation (n=3 biological replicates). The symbol $**p < 0.01$ represents statistical significance between the control and treated samples. The symbols $###p < 0.001$ and $##p < 0.01$ represent statistical significance between the indicated samples. On the right, immunoprecipitation experiment performed on secretome of cells incubated with IGFBP7 and Activin A. The proteins were immunoprecipitated with anti-IGFBP7 antibody and western blot was performed with anti-Activin A antibody. Input: western blot performed on proteins present in culture medium; SUP and IP indicate the supernatant and the immunoprecipitated components of immunoreaction, respectively. **(B)** SMAD pathways. Representative western blot analysis of nuclear and cytoplasmic levels of phosphorylated-SMAD2/3 (pSMAD2/3), SMAD2/3, phosphorylated-SMAD1/5 (pSMAD1/5), SMAD1/5 in cells incubated with IGFBP7 and/or Activin A. GAPDH and Histone 4 (H4) were used as cytoplasmic and nuclear markers, respectively. The histograms show the cytoplasmic and nuclear pSMAD2-3/SMAD2-3 and pSMAD1-5/SMAD1-5 ratios in the different experimental conditions. Data are expressed with standard deviation (n=3 biological replicates). In the histograms, the symbols on the white bars $***p < 0.001$ and $**p < 0.01$ represent a statistical significance between the control and treated samples; the symbols on the blue bars $###p < 0.001$ and $##p < 0.01$ represent a statistical significance between the control and treated samples. **(C)** On the left, representative immunoprecipitation experiment performed on secretome of cells incubated with IGFBP7. The proteins were immunoprecipitated with anti-IGFBP7 antibody and western blot was performed with anti-ACVR1 and anti-ACVR1B antibodies. Input: western blot performed on proteins present in secretome; SUP and IP indicate the supernatant and the immunoprecipitated components of immunoreaction, respectively. On the right, representative images of Duolink assay to identify physical proximity between IGFBP7 and ACVR1 and ACVR1B. The red dots represent a close interaction between IGFBP7 and ACVR1 or ACVR1B. The nuclei were DAPI stained with (blue). The scale bar corresponds to 100 microns

suggesting a compensatory mechanism to avoid excessive senescence. Notably, preliminary data indicate that IGFBP7, in addition to blocking Activin A, may interact with its receptors and induce senescence through SMAD pathways. Figure 4 provides an overview of the pleiotropic signaling pathways that IGFBP7 may use to promote cellular senescence.

This study identifies IGFBP7 as a key regulator in SASP-induced senescence. Notably, earlier research has shown that other IGFBPs, such as IGFBP4 and IGFBP5, can induce senescence in both cell cultures and living organisms. These studies position IGFBP proteins at the top of the signaling hierarchy governing the spread of senescence from primary senescent cells, i.e., those damaged by genotoxic agents, to surrounding healthy cells. It is important to note that IGFBP release relies on a common mechanism, as the ROS-prostaglandin pathway plays a role in the release of IGFBP4, IGFBP5, and IGFBP7.

In contrast, the induction of secondary senescence occurs through distinct and only partially overlapping pathways. IGFBP5 acts via caveolae internalization and interaction with the RAR α protein. IGFBP4 operates by modulating IGFII signaling, while IGFBP7, in addition to regulating IGFII circuits, also influences Insulin- and Activin-related pathways.

The observation that each of these three factors can induce senescence individually raises an important question: Why does the SASP contain all three proteins? It can be speculated that partially redundant and subsidiary molecular circuits may be necessary to ensure the onset of a robust senescence process in different cell types and under varying environmental conditions.

In conclusion, our findings highlight that IGFBP7, along with other members of the IGFBP family, plays a critical role in senescence-related signaling circuits. Therefore, these proteins may represent prime targets for anti-aging strategies aimed at reducing the burden of senescence on tissues and organs.

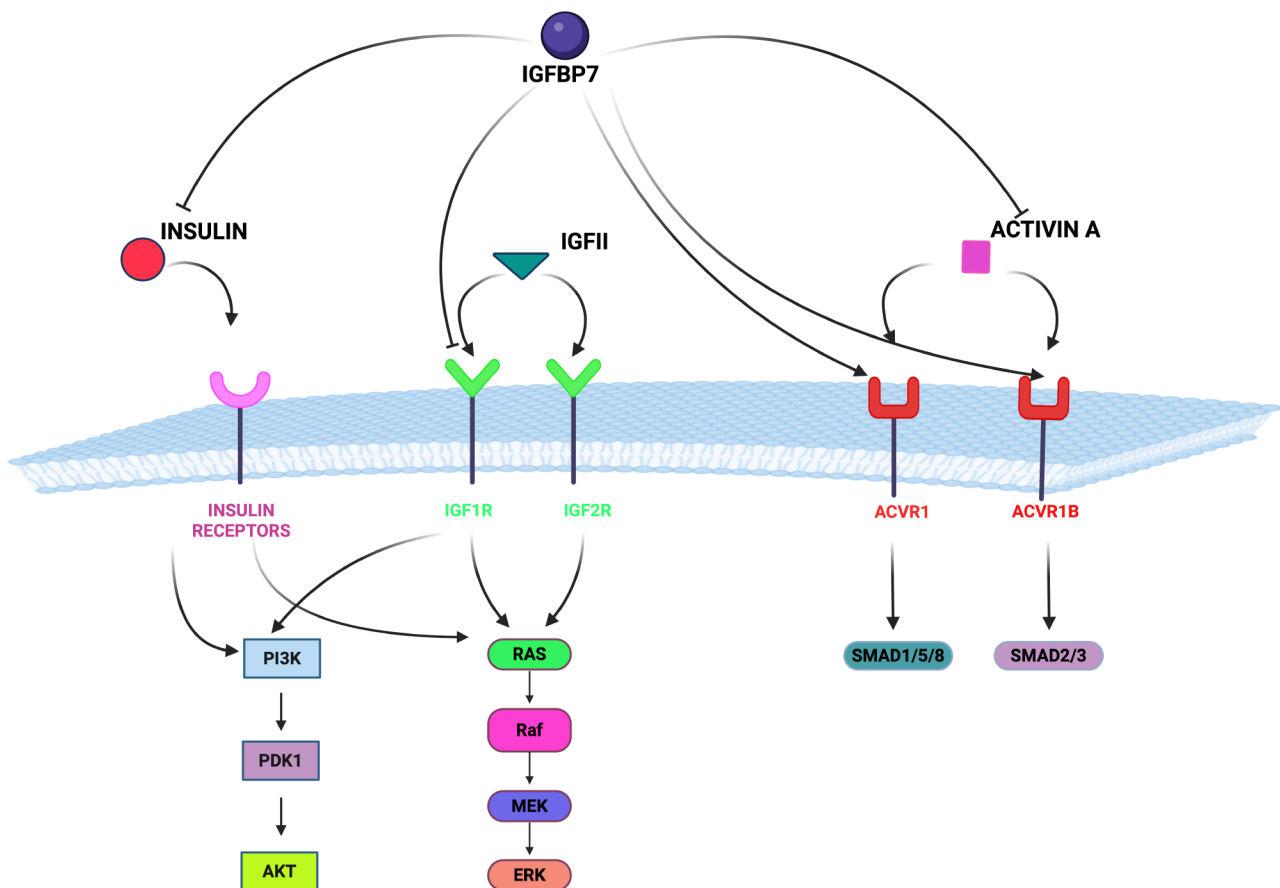


Fig. 4 IGFBP7 Signaling Associated with Senescence. The diagram presents a proposed model of pathways involved in senescence induced by IGFBP7 signaling. The IGFBP7 protein may interact with Insulin, preventing its interaction with cognate receptors and thereby inhibiting Insulin's anti-senescence and proliferative activities. IGFBP7 may also bind to the IGF1R receptor, redirecting IGF-II to IGF2R, which is associated with IGF-II-induced senescence. Additionally, IGFBP7 and Activin A may bind to each other, mutually blocking their respective pro-senescence activities. In the absence of Activin A, IGFBP7 may bind to ACVR1 and ACVR1B, promoting the onset of senescence

Materials and methods

MSC cultures

Bone marrow-derived MSCs were obtained from the American Type Culture Collection (ATCC PCS-500-012) and cultured in low glucose (1 g/L) DMEM supplemented with 3% human platelet lysates (PLT gold, cat. no. SCM151, Sigma-Aldrich, Saint Louis, MO, USA), 4 mM L-glutamine, 100 U/mL penicillin-streptomycin, and 5 ng/mL β FGF (PeproTech, Rock Hill, NJ, USA). Cells were seeded at a density of $1.0\text{--}2.5 \times 10^5$ cells/cm² in low glucose DMEM containing 10% FBS and β FGF, and cultured until they reached 80% confluency. The cells were then further propagated for the subsequent assays. Unless otherwise specified, all cell culture reagents were obtained from Euroclone Life Sciences (Pero, Italy).

Induction of acute senescence

MSCs at passage 3 were treated with hydrogen peroxide (H₂O₂) to induce acute senescence. Cells were incubated with 300 μ M H₂O₂ for 30 min in complete medium, followed by medium replacement and incubation for 48 h in fresh medium prior to further analysis.

Conditioned media (CM) preparation

After 48 h of acute senescence induction, CM was collected to evaluate IGFBP7 release and for other biological assays as described in the [Results](#) section. For CM preparation, the cultures were thoroughly washed with PBS 1x and transferred to a chemically defined, serum-free culture medium for overnight incubation. The CM was then collected for subsequent incubation with healthy MSC cultures. For western blot analysis, CM was concentrated using Amicon® Ultra Centrifugal Filters (10 kDa cutoff) and then the concentrated CM was evaluated as reported in “Western Blot Analysis” paragraph.

IGFBP7 neutralization in CM

IGFBP7 was immunodepleted in conditioned medium (CM) by incubating CM and cells with a polyclonal anti-human IGFBP7 antibody (Santa Cruz Biotechnology, Dallas, TX, USA; catalog no. sc363293) at a final concentration of 20 μ g/ml for 30 min at 4 °C. Following immunodepletion, healthy MSCs were cultured for 48 h at 37 °C in the antibody-treated CM. After the incubation period, cellular senescence was assessed using the Senescence-Associated β -Galactosidase assay (see below).

Effect of recombinant IGFBP7, IGF2, insulin, and activin A on MSC cultures

Recombinant human IGFBP7 (35 ng/ml), IGF2 (25 ng/ml), Activin A (100 ng/ml), and Insulin (1 μ g/ml) were added individually or in combination to MSC cultures. All reagents were obtained from PeproTech (Rock Hill, NJ, USA). Following treatment with these molecules,

senescence and other biological parameters were evaluated as described below.

Inhibition of PGE2 activation and antioxidant treatment

MSC cultures at passage 3 were incubated with 300 μ M H₂O₂ for 30 min in complete medium. After incubation, the medium was discarded, and the cells were incubated for 48 h in fresh medium with or without 200 μ M Parecoxib (Dynastat, Pharmacia Europe, UK) or with or without an antioxidant supplement (cat. no. A1345, Sigma-Aldrich, Saint Louis, MO, USA).

Immunocytochemistry and senescence-associated

β -Galactosidase

For the β -Galactosidase assay, 2×10^4 cells per well were seeded in 24-well plates with glass coverslips. After treatment, cells were fixed in 2% formaldehyde (Sigma-Aldrich, Saint Louis, MO, USA) for 10 min. The cells were then washed with PBS (Microgem, Napoli, Italy) and incubated at 37 °C overnight with a staining solution containing citric acid/phosphate buffer (pH 6), K₄Fe(CN)₆, K₃Fe(CN)₆, NaCl, MgCl₂, and X-Gal. Following staining, cells were permeabilized with 0.3% Triton-X100 (Roche, Basel, Switzerland) on ice for 5 min and then incubated in a blocking solution (5% FBS in PBS with 0.1% Triton-X100) for 1 h at room temperature (RT). Subsequently, samples were incubated overnight at 4 °C with an antibody against Ki67 (1:200, sc7846, Santa Cruz Biotechnology, Santa Cruz, CA, USA). The next day, a TRITC-conjugated secondary antibody (goat anti-mouse, 1:400, Gtx-Mu-003D594) from ImmunoReagents (Raleigh, NC, USA) was applied. Nuclear staining was performed using DAPI mounting medium (ab104139, Abcam, Cambridge, UK), and micrographs were captured using a Zeiss AxioScope 5 microscope equipped with an Axicam 305 digital camera (Zeiss Italy, Castiglione Olona, VA, Italy). The percentage of cells positive for β -Gal and Ki67 was calculated based on the number of cells expressing or not expressing the specific marker out of at least 500 cells in different microscopic fields.

Cell cycle analysis

For each analysis, 5×10^4 cells were collected by trypsin treatment and, after being washed with PBS, were fixed in 70% ethanol overnight at -20 °C. The samples were next washed with PBS and finally dissolved in a hypotonic buffer containing propidium iodide (Sigma-Aldrich, Saint Louis, MO, USA). The samples were acquired from a Guava EasyCyte flow cytometer (Merck Millipore, Danvers, MA, USA) and analyzed following a standard procedure using EasyCyte software.

Annexin V assay

Apoptosis was detected using a fluorescein-conjugated Annexin V kit (Dojindo Molecular Technologies, Munich, Germany) on a Guava EasyCyte flow cytometer (Sigma-Aldrich, Saint Louis, MO, USA) following the manufacturer's instructions. The kit has two different dyes (Annexin V and 7AAD) to identify apoptotic and non-apoptotic cells. Annexin V binds to phosphatidylserine on apoptotic cells, while 7AAD permeates and stains DNA of late-stage apoptotic and dead cells. The staining procedure allows the identification of 3 cell populations: non-apoptotic cells (Annexin V- and 7AAD-); early apoptotic cells (Annexin V+ and 7AAD-); late-apoptotic or dead cells (Annexin V+ and 7AAD+). In our experimental conditions, early and late apoptotic cells were grouped together.

Western blot (WB) analysis

Cells were lysed in a buffer containing 0.1% Triton (Bio-Rad, Irvine, CA, USA) for 30 min on ice. Next, 20 µg of each lysate was electrophoresed in a polyacrylamide gel and electroblotted onto a nitrocellulose membrane. We used the following primary antibodies: GAPDH (G8795) from Sigma-Aldrich (Saint Louis, MO, USA); IGFBP7 (sc-365293) IGFII (sc-5662), IGF1R (sc271606), IGF2R (sc-245462), Insulin (sc-8033), INSR (sc-57344), P21CIP1 (sc-6246), SMAD2/3 (sc-133098) were obtained from Santa Cruz Biotechnology (Dallas, TX, USA); ACVR1 (EAB-14737), ACVR1B (EAB-60969), ANNEXIN V (EAB-40440), BCL2 (EAB-22004), Histone H4 (EAB-11291), P16 (EAB-65673), P53 (EAB-20287), RB1 (EAB-32752), SMAD1/5 (EAB-92425) were obtained from Elabscience (Houston, TX, USA). AKT (#2920), phospho-AKT (#4060), ERK1/2 (#9102), phospho-ERK1/2 (#9106), phospho-SMAD2/3 (#8828), P38 (#9212) from Cell Signaling (Danver, MS, USA); RB2/P130 (BD610261) from BD Biosciences (San Jose, CA, USA); P27 (25614-1-AP) from Proteintech Europe (Manchester, UK). Immunoreactive signals were detected with a horseradish-peroxidase-conjugated secondary antibody (Elabscience, Houston, TX, USA) and reacted with ECL Plus reagent (Elabscience, Houston, TX, USA). All antibodies were used according to the manufacturer's instructions. Membrane staining with Ponceau S acid red was used as a loading control. The mean value was quantified densitometrically using Quantity One 1-D analysis software (Bio-Rad, Milan, Italy).

Immunoprecipitation

Immunoprecipitation assays were performed on MSC cell lysates, CM collected as described above, or culture media supplemented with 2 µg/ml IGFBP7 and Insulin. Cell lysates were prepared by incubating cells in a buffer containing 0.1% Triton X-100 (Bio-Rad, CA, USA)

for 30 min on ice. CM was concentrated using Amicon® Ultra Centrifugal Filters (10 kDa cutoff).

A total of 500 µL of concentrated CM or 500 ng of cell lysates were incubated with 2 µg of the corresponding antibodies for 4 h at 4 °C with gentle rotation. Subsequently, 30 µL of pre-washed protein A/G-conjugated agarose beads (MedChemExpress, NJ, USA) were added to the samples and incubated overnight. Proteins in the supernatant (sup) and pellet (IP) were separated by 12% SDS-PAGE under reducing conditions in Laemmli Buffer with boiling. The separated proteins were then transferred to a membrane, incubated with primary antibodies overnight, and detected using an Azure Biosystem.

The interaction between IGFBP7 and Insulin was evaluated by incubating 2 µg of each protein in DMEM at room temperature for several minutes, followed by immunoprecipitation as described above.

Duolink PLA fluorescence

Cells were grown on coverslips in a 24-well plate. The Duolink assay was performed according to the manufacturer's instructions (Sigma Aldrich, MO, USA), using IGFBP7 (Elabscience, TX, USA) with either ACVR1 (Elabscience, TX, USA) or ACVR1B (E-AB-93398, Elabscience, TX, USA) as primary antibodies. Micrographs were captured using a Zeiss Axioscope 5 microscope equipped with an Axicam 305 digital camera (Zeiss Italy, Castiglione Olona – VA, Italy).

Signaling pathways

IGF2, Insulin, and Activin A signal transduction can occur through various pathways. We aimed to identify which pathways might be associated with cellular senescence. MSC cultures were incubated at 37 °C for 30 min with each of the following inhibitors separately: 1 µM U0126 (ERK inhibitor, Sigma-Aldrich), 1 µM GSK690693 (AKT inhibitor, Sigma-Aldrich), 2 µg/ml anti-ACVR1 antibody (Elabscience), or 2 µg/ml anti-ACVR1B antibody (Elabscience). Subsequently, IGFBP7 was added, either alone or in combination with IGF2, Insulin, or Activin A, and the samples were further incubated for 24 h. Senescence assays and western blot analyses were then performed. Western blots were conducted on the nuclear and cytoplasmic fractions of MSC lysates. For this purpose, cells were incubated in a buffer containing 0.5% Nonidet P-40 for 5 min at 4 °C. The nuclear and cytosolic fractions were obtained by centrifugation at 500 g for 5 min. Each fraction was washed three times with lysis buffer, resuspended in lysis buffer, and further centrifuged at 17,500 g. Pellets were then subjected to western blot analysis.

mRNA extraction and real-time qPCR

Total RNA was extracted from cells using TRI Reagent (Molecular Research Center Inc., Cincinnati, OH, USA). RNA quantification was performed using a NanoDrop Spectrophotometer (Thermo Scientific, Waltham, MA, USA). Primer pairs for real-time qPCR were designed using OligoArchitect (Sigma-Aldrich). GAPDH mRNA was used as an internal control. Real-time PCR assays were conducted in triplicate using a LineGene 9600 Plus system (Bioer, Binjiang, Hangzhou, China) according to the manufacturer's instructions. SYBR Green PCR Master Mix (abm, Richmond, BC, Canada) was used, and the $2^{-\Delta\Delta CT}$ method was employed for relative quantification.

Statistical analysis

Statistical significance was evaluated using ANOVA followed by Student's t-test and Bonferroni's post-hoc test. Mixed-model variance analysis was employed for data with continuous outcomes. All data were analyzed using GraphPad Prism version 9 software (GraphPad, Boston, MA, USA).

Abbreviations

IGFs	Insulin growth factors
IGFBPs	Insulin growth factors
MSCs	Mesenchymal stromal cells
ROS	Reactive oxygen species
SASP	Senescence-associated secretory phenotype

Supplementary Information

The online version contains supplementary material available at <https://doi.org/10.1186/s12964-024-01921-2>.

Supplementary Material 1

Acknowledgements

Figure 4 contain images generated with Biorender licensed to U.G.

Author contributions

U.G. conceptualized research; U.G., N.A. and G.D. designed research; N.A., D.A., Y.S. performed research; N.A., G.P., and G.D. contributed new reagents/analytic tools; N. A., Y.S., D.A., G.P., G.D. and U.G. analyzed data; and N.A., Y.S. and U.G. wrote the paper.

Funding

The work presented herein was partly supported by grants from Regione Campania Progetto POR "iCURE" CUP B21C17000030007 awarded to U.G. Salary of Assistant Professor for N.A. was obtained from iCURE.

Data availability

All raw western blot images are provided in a Supplementary File.

Declarations

Ethics approval and consent to participate

N/A.

Consent for publication

N/A.

Competing interests

The authors declare no competing interests.

Author details

¹Department of Experimental Medicine, Luigi Vanvitelli Campania University, Naples, Italy

²Genome and Stem Cell Center (GENKÖK), Erciyes University, Kayseri, Turkey

³Sbarro Institute for Cancer Research and Molecular Medicine, Center for Biotechnology, Temple University, Philadelphia, PA, USA

⁴International Medical University UNICAMILLUS, Rome, Italy

⁵College of Medicine and Health Sciences, Bahir Dar University, Bahir Dar, Ethiopia

⁶Department of Experimental Medicine, Luigi Vanvitelli Campania University, Via Luigi De Crecchio 7, Napoli 80138, Italy

Received: 13 August 2024 / Accepted: 1 November 2024

Published online: 12 November 2024

References

1. Campisi J. Aging, cellular senescence, and cancer. *Annu Rev Physiol.* 2013;75:685–705.
2. Campisi J, d'Adda Di Fagagna F: Cellular senescence: when bad things happen to good cells. *Nat Rev Mol Cell Biol.* 2007;8:729–40.
3. Fridlyanskaya I, Alekseenko L, Nikolsky N. Senescence as a general cellular response to stress: a mini-review. *Exp Gerontol.* 2015;72:124–8.
4. Herranz N, Gil J. Mechanisms and functions of cellular senescence. *J Clin Invest.* 2018;128:1238–46.
5. Hao X, Wang C, Zhang R. Chromatin basis of the senescence-associated secretory phenotype. *Trends Cell Biol.* 2022;32:513–26.
6. Schafer MJ, Zhang X, Kumar A, Atkinson EJ, Zhu Y, Jachim S, Mazula DL, Brown AK, Berning M, Aversa Z et al. The senescence-associated secretome as an indicator of age and medical risk. *JCI Insight* 2020, 5.
7. van Deursen JM. The role of senescent cells in ageing. *Nature.* 2014;509:439–46.
8. Baxter RC. IGF binding proteins in cancer: mechanistic and clinical insights. *Nat Rev Cancer.* 2014;14:329–41.
9. Kenyon C. A conserved regulatory system for aging. *Cell.* 2001;105:165–8.
10. Oguma Y, Alessio N, Aprile D, Dezawa M, Peluso G, Di Bernardo G, Galderisi U. Meta-analysis of senescent cell secretomes to identify common and specific features of the different senescent phenotypes: a tool for developing new senotherapeutics. *Cell Commun Signal.* 2023;21:262.
11. Alessio N, Aprile D, Peluso G, Mazzone V, Patrone D, Di Bernardo G, Galderisi U. IGFBP5 is released by senescent cells and is internalized by healthy cells, promoting their senescence through interaction with retinoic receptors. *Cell Commun Signal.* 2024;22:122.
12. Alessio N, Squillaro T, Di Bernardo G, Galano G, De Rosa R, Melone MA, Peluso G, Galderisi U. Increase of circulating IGFBP-4 following genotoxic stress and its implication for senescence. *Elife* 2020, 9.
13. Jin L, Shen F, Weinfeld M, Sergi C. Insulin growth factor binding protein 7 (IGFBP7)-Related Cancer and IGFBP3 and IGFBP7 crosstalk. *Front Oncol.* 2020;10:727.
14. Akiel M, Rajasekaran D, Gredler R, Siddiq A, Srivastava J, Robertson C, Jariwala NH, Fisher PB, Sarkar D. Emerging role of insulin-like growth factor-binding protein 7 in hepatocellular carcinoma. *J Hepatocell Carcinoma.* 2014;1:9–19.
15. Grotendorst GR, Lau LF, Perbal B. CCN proteins are distinct from, and should not be considered members of, the insulin-like growth factor-binding protein superfamily. *J Clin Endocrinol Metab.* 2001;86:944–5.
16. Yamanaka Y, Wilson EM, Rosenfeld RG, Oh Y. Inhibition of insulin receptor activation by insulin-like growth factor binding proteins. *J Biol Chem.* 1997;272:30729–34.
17. Haridoss S, Yovchev MI, Schweizer H, Megherhi S, Beecher M, Locker J, Oertel M. Activin A is a prominent autocrine regulator of hepatocyte growth arrest. *Hepatol Commun.* 2017;1:852–70.
18. Harrington AE, Morris-Triggs SA, Ruotolo BT, Robinson CV, Ohnuma S, Hyvonen M. Structural basis for the inhibition of activin signalling by follistatin. *EMBO J.* 2006;25:1035–45.
19. Kato MV. A secreted tumor-suppressor, mac25, with activin-binding activity. *Mol Med.* 2000;6:126–35.

20. de Kretser DM, O'Hehir RE, Hardy CL, Hedger MP. The roles of activin A and its binding protein, follistatin, in inflammation and tissue repair. *Mol Cell Endocrinol*. 2012;359:101–6.
21. Galderisi U, Peluso G, Di Bernardo G. Clinical trials based on mesenchymal stromal cells are exponentially increasing: where are we in recent years? *Stem Cell Rev Rep*. 2022;18:23–36.
22. Qiu B, Chu LY, Li XX, Peng YH, Xu YW, Xie JJ, Chen XY. Diagnostic value of serum insulin-like growth factor binding protein 7 (IGFBP7) in Colorectal Cancer. *Oncotargets Therapy*. 2020;13:12131–9.
23. Szyszkowska A, Baranska S, Sawicki R, Tarasiuk E, Dubatówka M, Kondraciuk M, Sawicka-Smiarowska E, Knapp M, Glowinski J, Kaminski K, Lisowska A. Insulin-like growth factor-binding protein 7 (IGFBP-7)-New diagnostic and prognostic marker in symptomatic peripheral arterial disease?-Pilot study. *Biomolecules* 2022, 12.
24. Ruvolo PP, Deng X, May WS. Phosphorylation of Bcl2 and regulation of apoptosis. *Leukemia*. 2001;15:515–22.
25. Fang S, Wang J, Liu G, Qu B, Chunyu J, Xu W, Xiang J, Li X. DPPA2/4 promote the pluripotency and proliferation of bovine extended pluripotent stem cells by upregulating the PI3K/AKT/GSK3beta/beta-Catenin signaling pathway. *Cells* 2024, 13.
26. Kashyap V, Rezende NC, Scotland KB, Shaffer SM, Persson JL, Gudas LJ, Mongan NP. Regulation of stem cell pluripotency and differentiation involves a mutual regulatory circuit of the NANOG, OCT4, and SOX2 pluripotency transcription factors with polycomb repressive complexes and stem cell microRNAs. *Stem Cells Dev*. 2009;18:1093–108.
27. Kaneko K, Walker SL, Lai-Cheong J, Matsui MS, Norval M, Young AR. cis-urocanic acid enhances prostaglandin E2 release and apoptotic cell death via reactive oxygen species in human keratinocytes. *J Invest Dermatol*. 2011;131:1262–71.
28. Miller SB. Prostaglandins in health and disease: an overview. *Semin Arthritis Rheum*. 2006;36:37–49.
29. Passos JF, Nelson G, Wang C, Richter T, Simillion C, Proctor CJ, Miwa S, Olijslagers S, Hallinan J, Wipat A, et al. Feedback between p21 and reactive oxygen production is necessary for cell senescence. *Mol Syst Biol*. 2010;6:347.
30. Shao L, Li H, Pazhanisamy SK, Meng A, Wang Y, Zhou D. Reactive oxygen species and hematopoietic stem cell senescence. *Int J Hematol*. 2011;94:24–32.
31. Wang T, Qin L, Liu B, Liu Y, Wilson B, Eling TE, Langenbach R, Taniura S, Hong JS. Role of reactive oxygen species in LPS-induced production of prostaglandin E2 in microglia. *J Neurochem*. 2004;88:939–47.
32. Aravinthan A, Challis B, Shannon N, Hoare M, Heaney J, Alexander GJM. Selective insulin resistance in hepatocyte senescence. *Exp Cell Res*. 2015;331:38–45.
33. Barinda AJ, Ikeda K, Nugroho DB, Wardhana DA, Sasaki N, Honda S, Urata R, Matoba S, Hirata KI, Emoto N. Endothelial progeria induces adipose tissue senescence and impairs insulin sensitivity through senescence associated secretory phenotype. *Nat Commun*. 2020;11:481.
34. Matsui-Hirai H, Hayashi T, Yamamoto S, Ina K, Maeda M, Kotani H, Iguchi A, Ignarro LJ, Hattori Y. Dose-dependent modulatory effects of insulin on glucose-induced endothelial senescence in vitro and in vivo: a relationship between telomeres and nitric oxide. *J Pharmacol Exp Ther*. 2011;337:591–9.
35. Evdokimova V, Tognon CE, Benatar T, Yang W, Krutikov K, Pollak M, Sorensen PH, Seth A. IGFBP7 binds to the IGF-1 receptor and blocks its activation by insulin-like growth factors. *Sci Signal*. 2012;5:ra92.
36. Clayton PE, Banerjee I, Murray PG, Renehan AG. Growth hormone, the insulin-like growth factor axis, insulin and cancer risk. *Nat Rev Endocrinol*. 2011;7:11–24.
37. Zhao Y, Wu Z, Chanal M, Guillaumond F, Goehrig D, Bachy S, Principe M, Ziv-erec A, Flaman JM, Collin G, et al. Oncogene-induced senescence limits the progression of pancreatic neoplasia through production of activin A. *Cancer Res*. 2020;80:3359–71.
38. Aykul S, Corpina RA, Goebel EJ, Cunanan CJ, Dimitriou A, Kim HJ, Zhang Q, Rafique A, Leidich R, Wang X et al. Activin a forms a non-signaling complex with ACVR1 and type II Activin/BMP receptors via its finger 2 tip loop. *Elife* 2020, 9.
39. Olsen OE, Sankar M, Elsaadi S, Hella H, Buene G, Darvekar SR, Misund K, Katagiri T, Knaus P, Holien T. BMPR2 inhibits activin and BMP signaling via wild-type ALK2. *J Cell Sci* 2018, 131.
40. Graham H, Peng C. Activin receptor-like kinases: structure, function and clinical implications. *Endocr Metab Immune Disord Drug Targets*. 2006;6:45–58.
41. Dagouassat M, Gagliolo JM, Chrusciel S, Bourin MC, Duprez C, Caramelle P, Boyer L, Hue S, Stern JB, Validire P, et al. The Cyclooxygenase-2-Prostaglandin E pathway maintains Senescence of Chronic Obstructive Pulmonary Disease fibroblasts. *Am J Respir Crit Care Med*. 2013;187:703–14.
42. Wiley CD, Sharma R, Davis SS, Lopez-Dominguez JA, Mitchell KP, Wiley S, Alimirah F, Kim DE, Payne T, Rosko A, et al. Oxylipin biosynthesis reinforces cellular senescence and allows detection of senolysis. *Cell Metabol*. 2021;33:1124–.

Publisher's note

Springer Nature remains neutral with regard to jurisdictional claims in published maps and institutional affiliations.